Electronic Supplementary Material (ESI) for CrystEngComm.

Supporting Information

Designed synthesis of a turn-off fluorescence sensor based on a multifunctional Zn(II) coordination polymer for detection of Fe^{3+}, Hg^{2+} and 4-nitrophenol

Bo Zhao,[a] Jiangfeng Lu,[a] Hao Liu[a], Senlin Li,[a] Qiaozhen Sun,[a,*] Bingguang Zhang[b,*]

[a]*School of Materials Science and Engineering, Central South University, Changsha, 410083, China*

Email: rosesunqz@csu.edu.cn

[b]*Key Laboratory of Catalysis and Materials Sciences of the State Ethnic Affairs Commission & Ministry of Education, College of Chemistry and Material Science, South-Central Minzu University, Wuhan, 430074, China*

Email: zhangbg68@yahoo.com

*These authors contributed equally to this work.

Contents

Section 1 Synthesis of H_2L

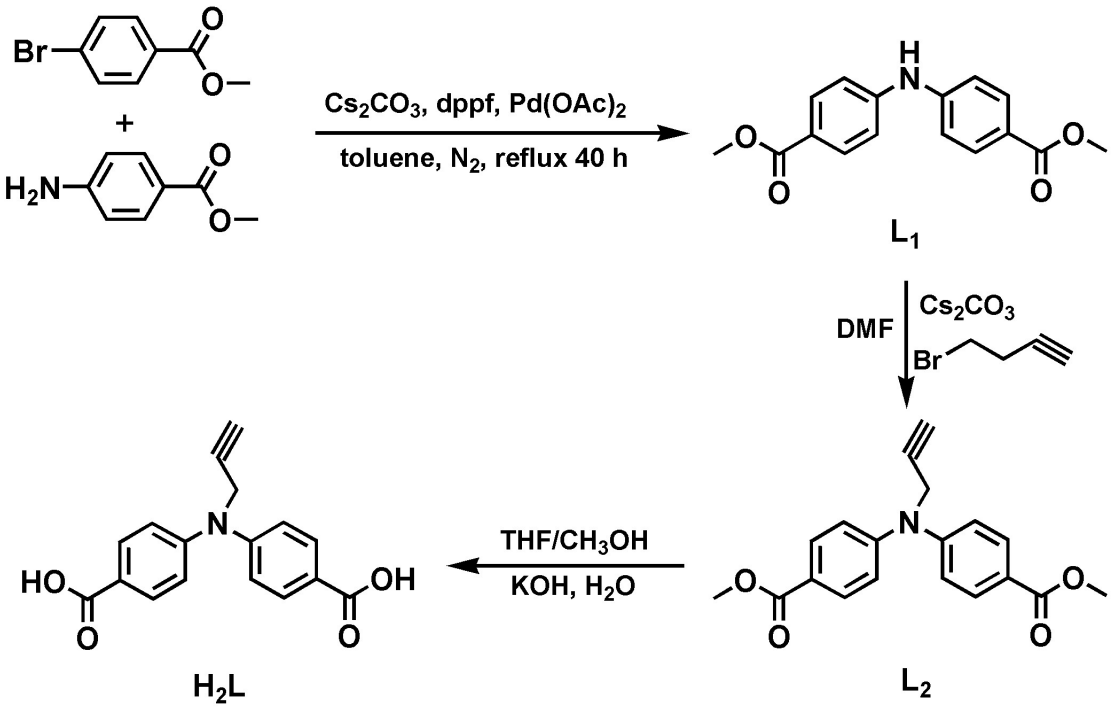

dppf: 1,1'-Bis(diphenylphosphino)ferrocene

Scheme S1. Synthetic route of H_2L ligand

Step 1

Syntheisis of L_1 (1,1'-Dimethyl 4,4'-iminobis[benzoate])**:** A mixture of 1-bromo-4-(methoxycarbonyl)benzene (21.5 g, 0.10 mol), (4-(methoxycarbonyl)phenyl)amine (18.1 g, 0.12 mol), Cs_2CO_3 (45.6 g, 0.14 mol), 1,1'-bis(diphenyphosphino)ferrocene (2.2 g, 4.0 mmol) and $Pd(OAc)_2$ (1.0 g, 4.4 mmol) in 800 mL toluene were refluxed 40 h under N_2 atmosphere. The solution was filtered and cooled to room temperature. The crystalline powder L_1 was separated and washed in a yield 17.1 g (~60%). ^{1}NMR (500 MHz, CD_3SOCD_3) δ (ppm): 9.28 (s, 1H), 7.89 (m, 4H), 7.24 (m, 4H), 3.81 (s, 6H).

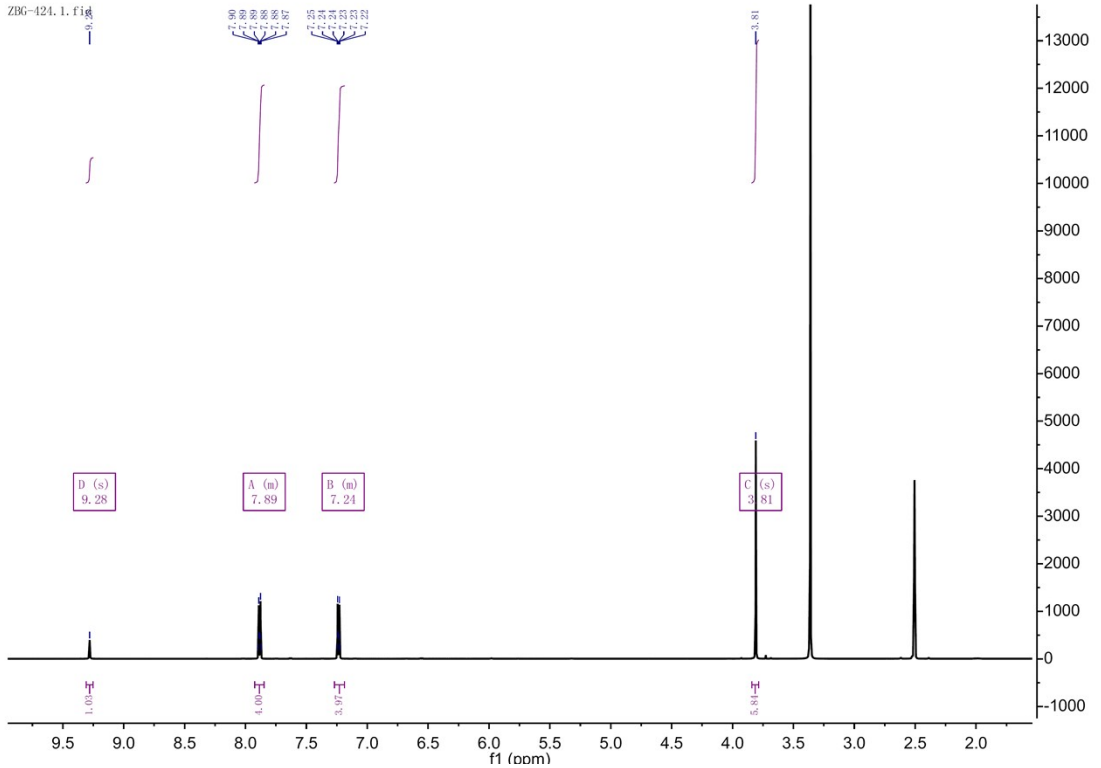

Step 2

Syntheisis of L_2 (4,4'-(ethynylimino)bis[benzoate])**:** A mixture of L_1 (7.1 g, 25 mmol), Cs_2CO_3 (16.3 g, 50 mmol) and 3-bromo-1-propyne (3.0 g, 25 mmol) in 60 mL dry DMF were stirred at room temperature for one night. The solution was filtered and the solvent was removed under reduced pressure. The crude product was washed with water and separated by silica gel column chromatorgraphy (CH_2Cl_2) to afford L_2. ^{1}NMR (500 MHz, $CDCl_3$) δ (ppm): 8.00 (m, 4H), 7.14 (m, 4H), 4.50 (d, 2H), 3.90 (s, 6H), 2.28 (t, 1H).

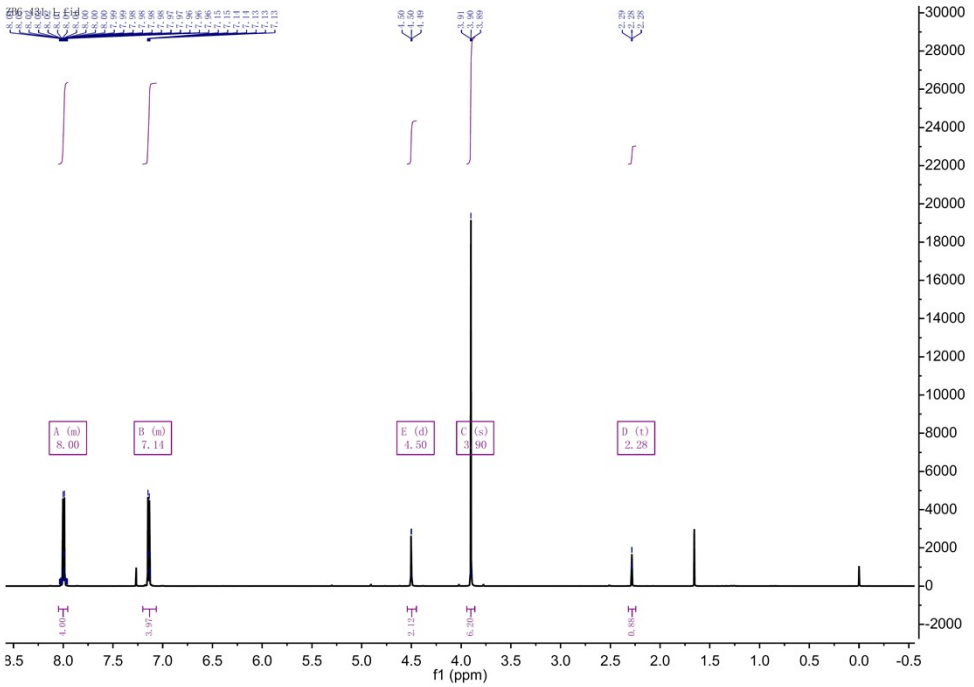

Step 3

Synthesis of H_2L (4,4'-(ethynylimino)bis[benzoic acid])**:** L_2 (5.8 g, 18 mmol) was dissolved in 180 mL THF/CH_3OH mixed solution. Then KOH solution was added and stirred for one night at room temperature. The solution was filtered and the solvent was removed under reduced pressure to afford H_2L. ^{1}NMR (500 MHz, CD_3SOCD_3) δ (ppm): 12.71 (s, 2H), 7.90 (m, 4H), 7.19 (m, 4H), 4.64 (d, 2H), 3.28 (t, 1H).

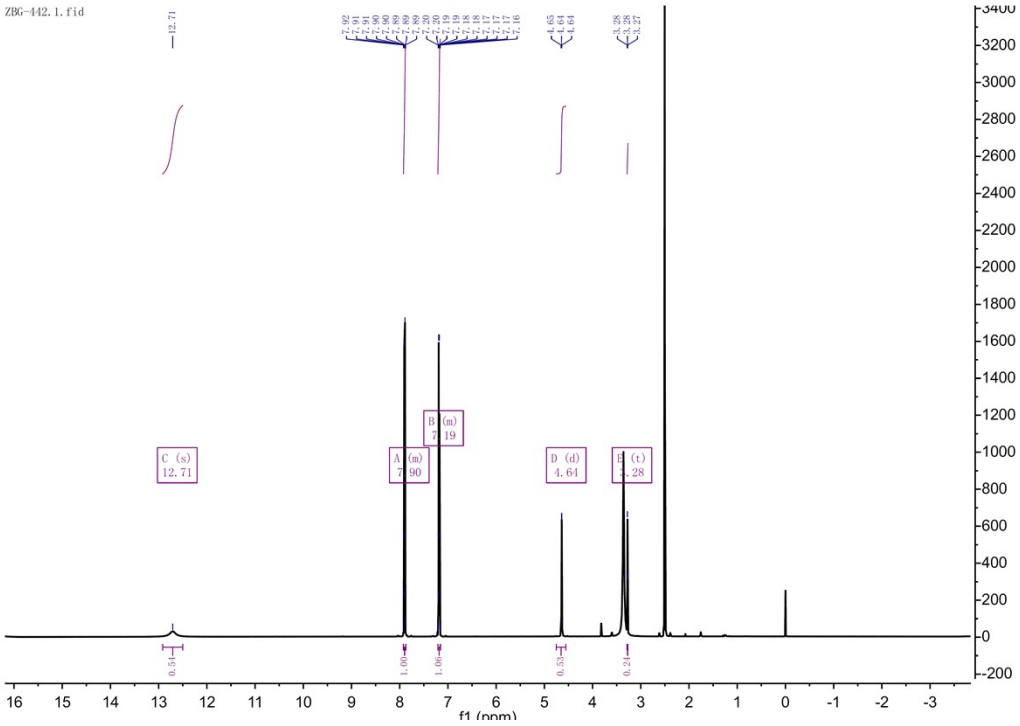

Section 2 General characterizations and structural information

Table S1 Selected Bond Lengths (Å) and Bond Angles (°) for **H_2L** and **1**

H_2L			
N(1)-C(10)	1.389(3)	N(1)-C(3)	1.430(3)
N(1)-C(1)	1.472(3)	O(1)-C(9)	1.225(3)
O(2)-C(9)	1.308(3)	O(3)-C(16)	1.283(4)
O(4)-C(16)	1.246(4)	C(1)-C(2)	1.474(4)
C(2)-C(17)	1.165(4)	C(3)-C(8)	1.375(3)
C(3)-C(4)	1.391(4)	C(4)-C(5)	1.377(4)
C(5)-C(6)	1.389(3)	C(6)-C(7)	1.380(4)
C(6)-C(9)	1.479(4)	C(7)-C(8)	1.376(4)
C(10)-C(15)	1.395(4)	C(10)-C11)	1.395(4)
C(11)-C(12)	1.390(4)	C(12)-C(13)	1.380(4)
C(13)-C(14)	1.386(4)	C(13)-C(16)	1.491(4)
C(14)-C(15)	1.370(4)	C(10)-N(1)-C(3)	121.1(2)
C(10)-N(1)-C(1)	121.8(2)	C(3)-N(1)-C(1)	116.0(2)
N(1)-C(1)-C(2)	112.6(2)	C(17)-C(2)-C(1)	176.8(3)
C(8)-C(3)-C(4)	119.6(2)	C(8)-C(3)-N(1)	120.4(2)
C(4)-C(3)-N(1)	120.0(2)	C(5)-C(4)-C(3)	120.1(2)
C(4)-C(5)-C(6)	120.2(3)	C(7)-C(6)-C(5)	119.1(2)
C(7)-C(6)-C(9)	121.8(2)	C(5)-C(6)-C(9)	119.1(2)
C(8)-C(7)-C(6)	120.8(2)	C(3)-C(8)-C(7)	120.1(2)
O(1)-C(9)-O(2)	122.6(2)	O(1)-C(9)-C(6)	123.0(2)
O(2)-C(9)-C(6)	114.4(2)	N(1)-C(10)-C(15)	120.9(2)
N(1)-C(10)-C(11)	121.5(2)	C(15)-C(10)-C(11)	117.6(3)
C(12)-C(11)-C(10)	120.2(3)	C(13)-C(12)-C(11)	121.5(3)
C(12)-C(13)-C(14)	118.1(3)	C(12)-C(13)-C(16)	122.5(3)
C(14)-C(13)-C(16)	119.3(3)	C(15)-C(14)-C(13)	120.9(3)
C(14)-C(15)-C(10)	121.6(3)	O(4)-C(16)-O(3)	124.1(3)

O(4)-C(16)-C(13)	120.3(3)	O(3)-C(16)-C(13)	115.6(3)
1			
Zn(1)-O(4)#1	1.938(9)	Zn(1)-O(1)	2.011(3)
Zn(1)-N(4)#2	2.073(3)	Zn(1)-N(2)	2.076(3)
Zn(1)-O(2)	2.492(3)	O(4)#1-Zn(1)-O(1)	125.1(5)
O(4)#1-Zn(1)-N(4)#2	107.4(4)	O(1)-Zn(1)-N(4)#2	97.74(11)
O(4)#1-Zn(1)-N(2)	125.3(5)	O(1)-Zn(1)-N(2)	100.30(12)
N(4)#2-Zn(1)-N(2)	93.21(12)	O(4)#1-Zn(1)-O(2)	93.1(4)
O(1)-Zn(1)-O(2)	57.01(9)	N(4)#2-Zn(1)-O(2)	154.26(11)
N(2)-Zn(1)-O(2)	87.32(11)		

Symmetry codes: (**1**) #1: -x+1, y+1, -z+1/2; #2: -x+3/2, y+1/2, -z+3/2.

Table S2 Hydrogen bond distances (Å) and bond angles (°) for **1** and **2**

D-H···A	d(D-H)	d(H…A)	d(D…A)	∠(DHA)
H_2L				
O(2)-H(2A)…O(1)#1	0.82	1.83	2.650(4)	178
O(3)-H(3A)…O(4)#2	0.82	1.81	2.626(3)	174
1				
N(3)-H (3)...O(2)#3	0.86	1.93	2.744(5)	159
C(24)-H(24) ...O(3)#4	0.93	2.21	3.047(4)	150

Symmetry codes: (**1**) #1: -x+2, -y-1, -z; #2: -x, -y+2, -z+1; #3: -x+3/2, -y+3/2, -z+1; #4: x+1/2, y+1/2, z+1.

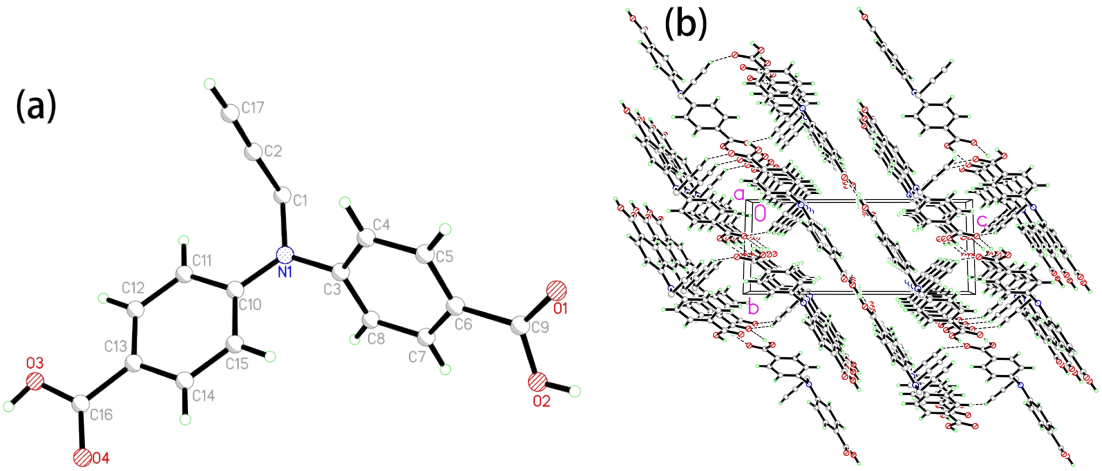

Fig. S1 The unit structure (a) and the packing diagram (b) of H_2L. The hydrogen bonds are shown in dashed lines.

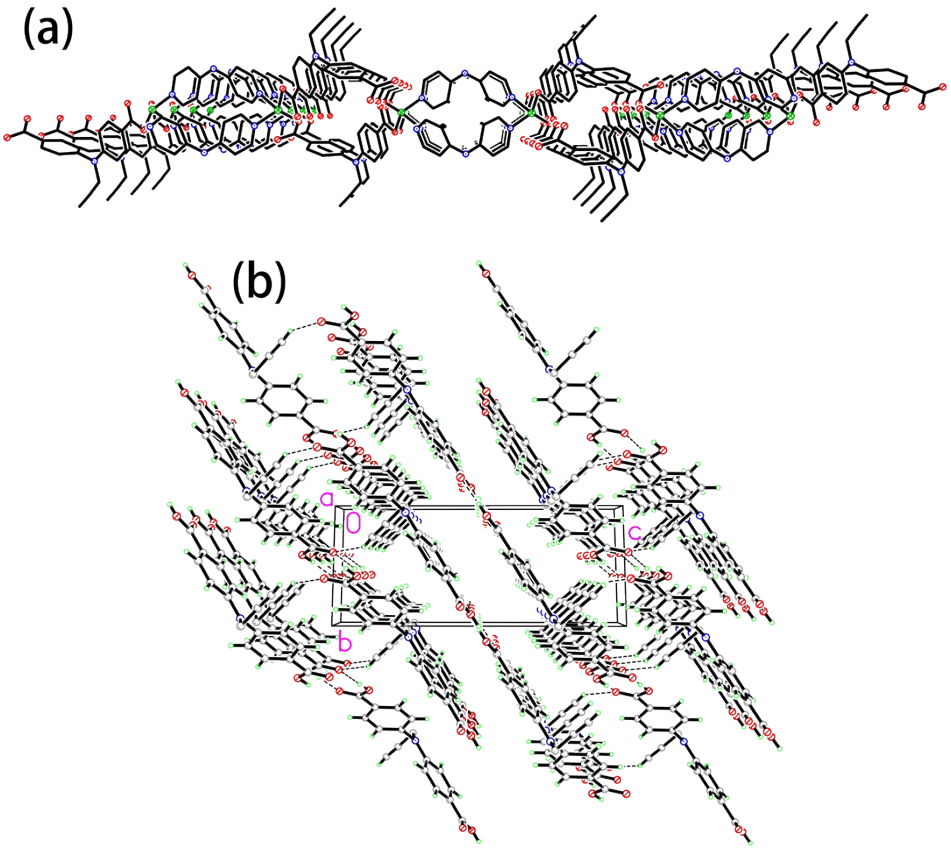

Fig. S2 (a) The 2D layer along *b* axis; (b) The packing diagram of **1**. The hydrogen bonds are shown in dashed lines.

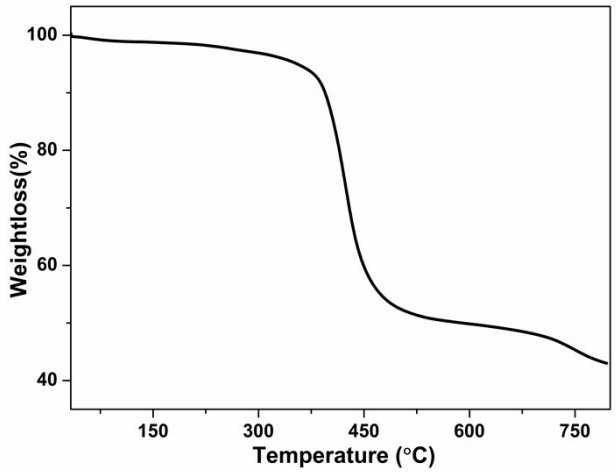

Fig. S3 The thermal analysis curve of compound **1**.

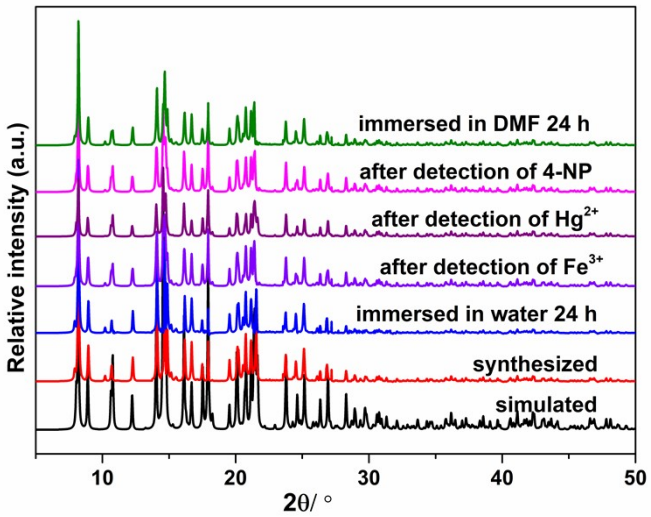

Fig. S4 PXRD pattern of compound **1**, the immersed sample and the detection of Fe^{3+}, Hg^{2+} and 4-NP.

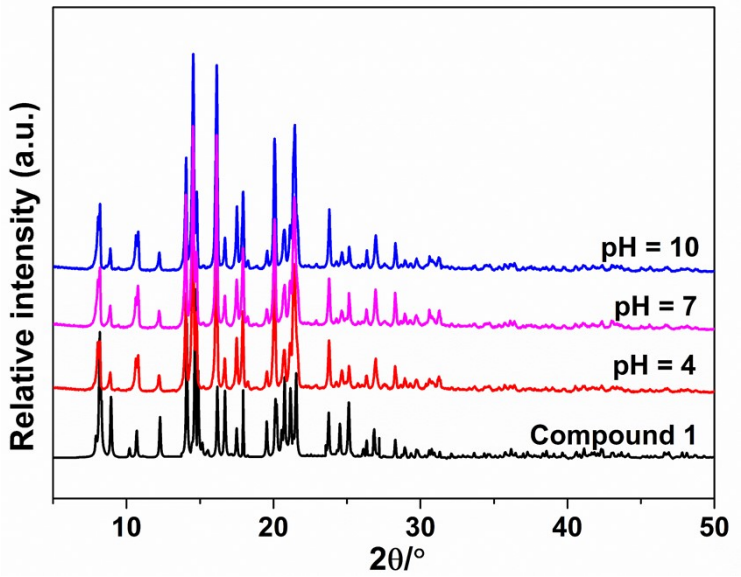

Fig. S5 The PXRD pattern of **1** after being soaked in acidic and basic solutions.

Section 3 Detection of Fe^{3+} and Hg^{2+}

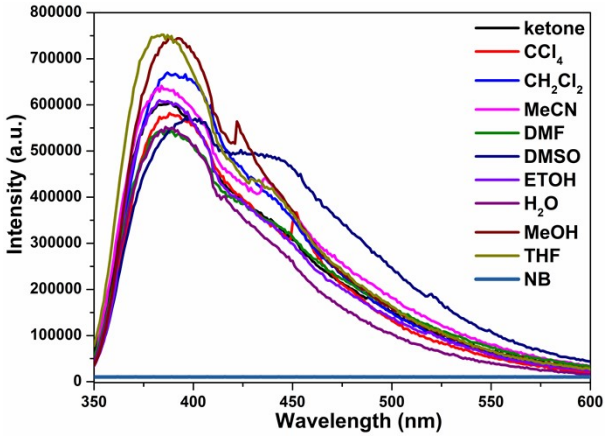

Fig. S6 Luminescent spectra of **1** (λ_{ex}: 320 nm) in different solvents (Condition: 5 mg **1**, 3 mL solvent).

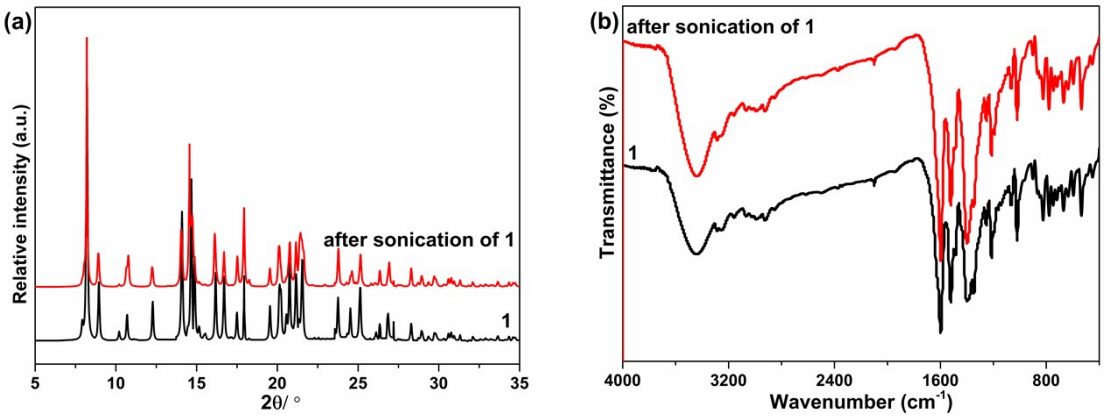

Fig. S7 PXRD pattern and IR spectra of compound **1** before and after sonication in water.

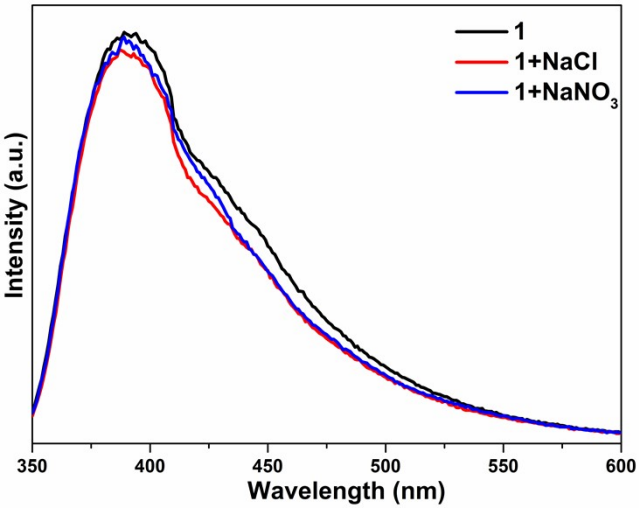

Fig. S8 The emission spectra of **1** immersed in water solution of NaCl and $NaNO_3$, respectively (Condition: 5 mg **1**, 3 mL H_2O and 0.02 mmol Na^+ ion).

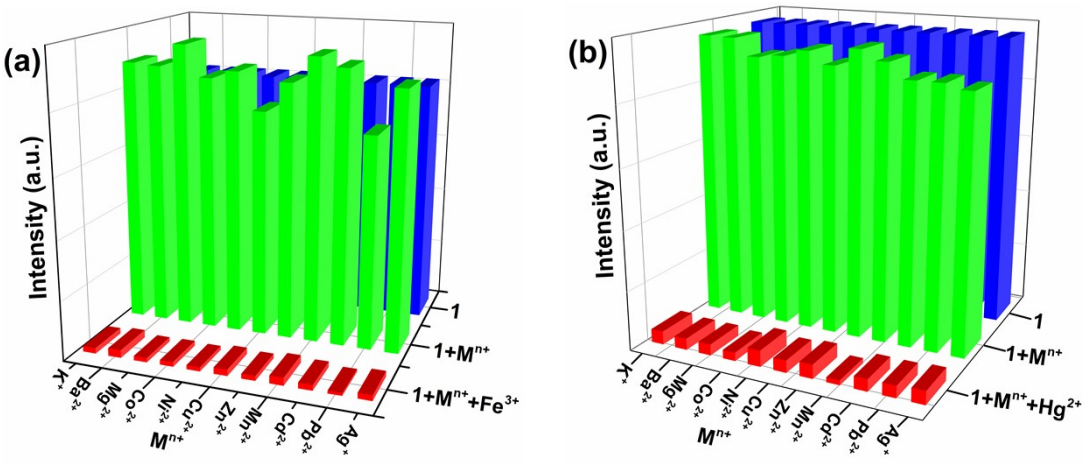

Fig. S9 The competition experiments of **1** for detection of (a) Fe^{3+} and (b) Hg^{2+} ions in the presence of the interfering metal cations (Condition: 5 mg MOF, 3 mL H_2O, 10 μL M^{n+} ions (0.1 M) and 10 μL Fe^{3+} (Hg^{2+}) (0.01 M)).

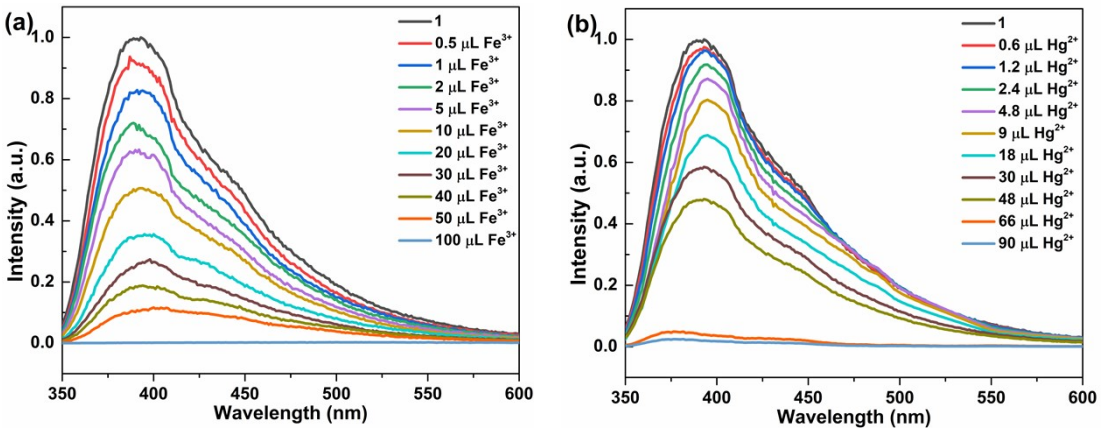

Fig. S10 Fluorescent spectra of **1** suspension (1.67 mg/mL) upon incremental addition of (a) Fe^{3+} and (b) Hg^{2+} (0.01 M).

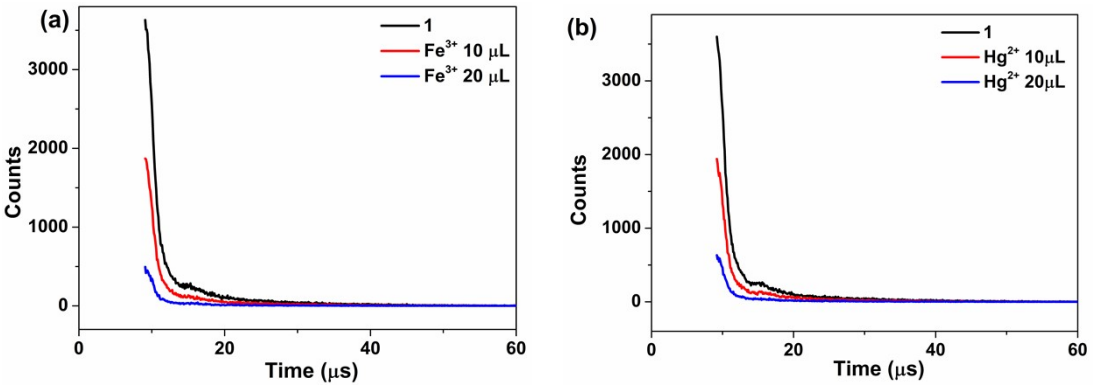

Fig. S11 The fluorescence decay curves of **1** in Fe^{3+} (a) and Hg^{2+} (b) solution (0.01 M).

Table S3 Average fluorescence lifetime (<τ>) values of **1** before and after addition of Fe^{3+} and Hg^{2+}, respectively

	a_1	a_2	τ_1 (μs)	τ_2 (μs)	<τ> (μs)	χ^2
Volume of Fe^{3+} solution added (μL, 0.01 M)						
0	4.23	0.37	1.08	9.15	4.51	1.17
10	2.37	0.16	1.22	9.56	4.11	1.17
20	0.56	0.043	1.00	8.47	3.94	0.94
Volume of Hg^{2+} solution added (μL, 0.01 M)						
0	4.53	0.32	1.24	9.95	4.39	1.09
10	2.19	0.19	1.05	8.00	3.81	1.02
20	0.75	0.06	1.10	8.83	3.54	1.16

$\langle\tau\rangle = (a_1\tau_1^2 + a_2\tau_2^2)/(a_1\tau_1 + a_2\tau_2)$

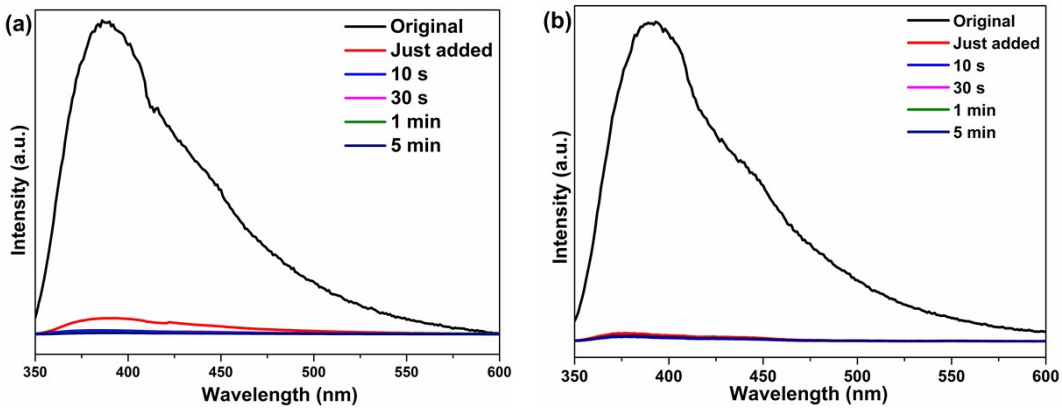

Fig. S12 Time-dependent fluorescent quenching detections of **1** for Fe^{3+} (a) and Hg^{2+} (b) ions.

To calculate the standard deviation and detection limit of this detection method, 5 mg **1** was well ground and suspended in 3 mL H_2O. Then, Fe^{3+} (Hg^{2+}) ion solution (0.01 M) was added into the suspension and the fluorescent intensities were recorded. Standard deviation (σ) was calculated from five blank tests of **1** suspension and the detection limit was calculated via the formula: 3σ/k (k: slope of the straight line).

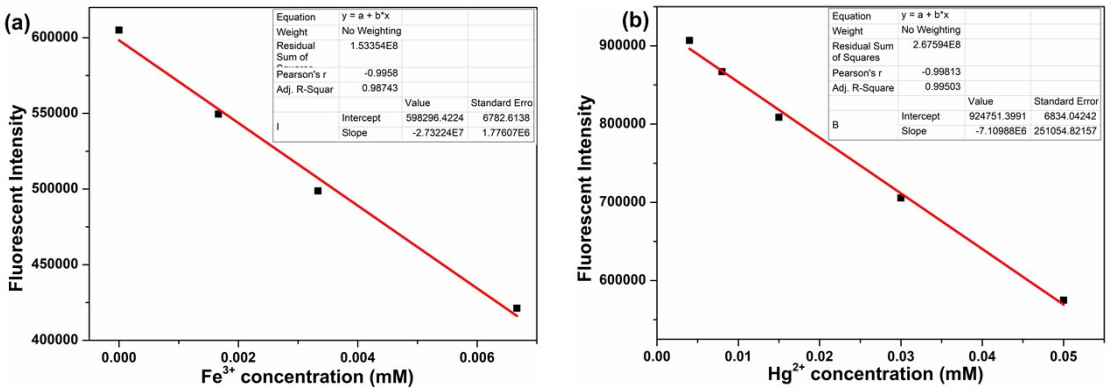

Fig. S13 Linear curve of fluorescent intensity of **1** suspension upon incremental addition of (a) Fe^{3+} and (b) Hg^{2+}.

Table S4 Standard deviation calculation

	Fluorescent intensity ($\times 10^5$)
Fe^{3+}	
Test 1	6.050
Test 2	6.072
Test 3	6.045
Test 4	6.076
Test 5	6.035
Standard deviation (σ)	0.0177
Hg^{2+}	
Test 1	10.001
Test 2	9.988
Test 3	9.998
Test 4	9.979
Test 5	9.996
Standard deviation (σ)	0.0089

Table S5 Detection limit calculation for Fe^{3+} and Hg^{2+}

Compound **1**	
Fe^{3+}	
Slope (k)	2.732×10^7 mM^{-1}
Detection limit (3σ/k)	0.000194 mM
Hg^{2+}	
Slope (k)	7.110×10^6 mM^{-1}
Detection limit (3σ/k)	0.000375 mM

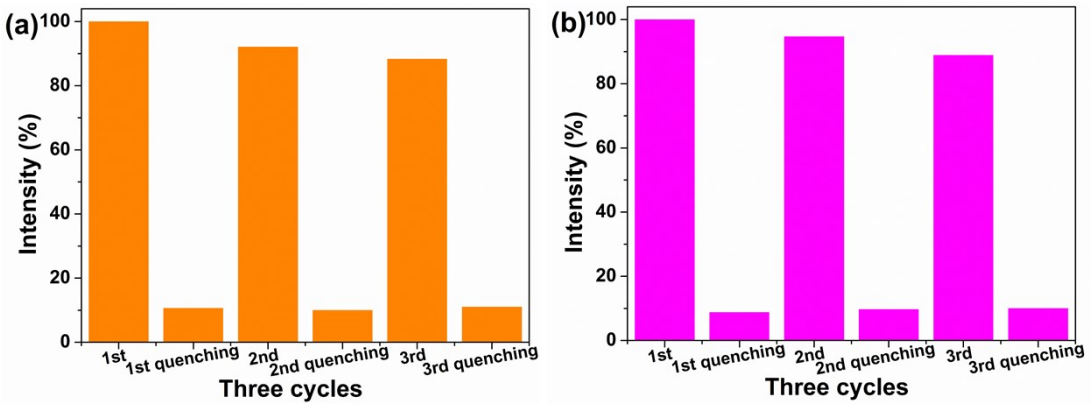

Fig. S14 Three quenching cycles of **1** suspension after addition of Fe^{3+} (a) and Hg^{2+} (b).

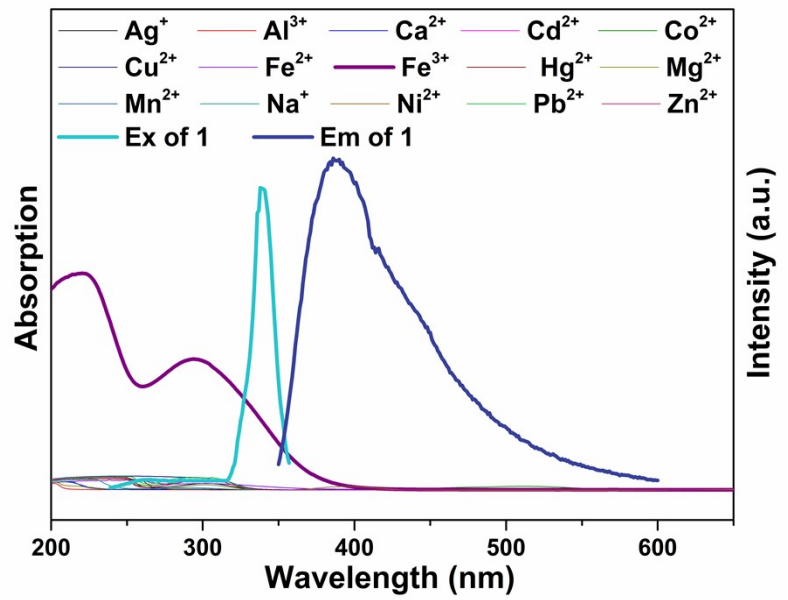

Fig. S15 UV−vis spectra of metal salts, the excitation and emission spectra of **1**, showing their overlapping.

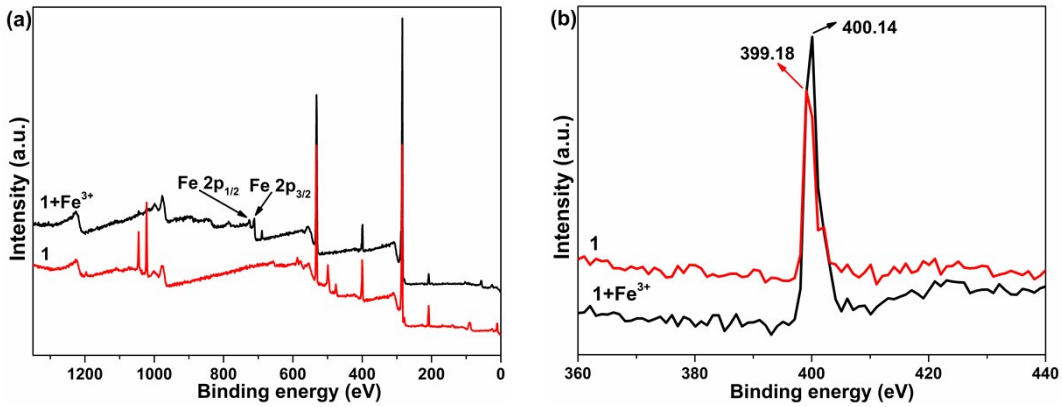

Fig. S16 (a) XPS for complex **1** and Fe^{3+} incorporating **1**; (b) N 1s XPS for **1** and Fe^{3+} incorporating **1**.

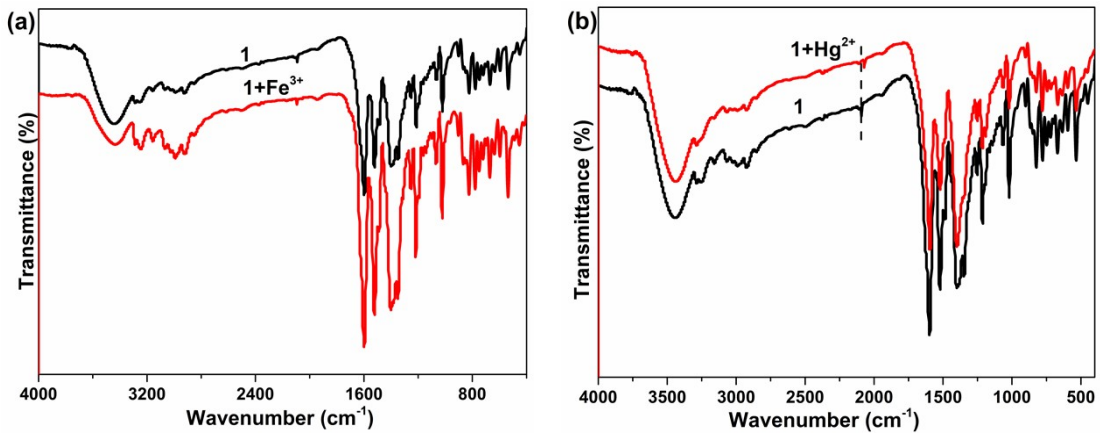

Fig. S17 (a) FT-IR spectra for complex **1** and Fe^{3+} incorporated **1**; (b) FT-IR spectra for complex **1** and Hg^{2+} incorporated **1**.

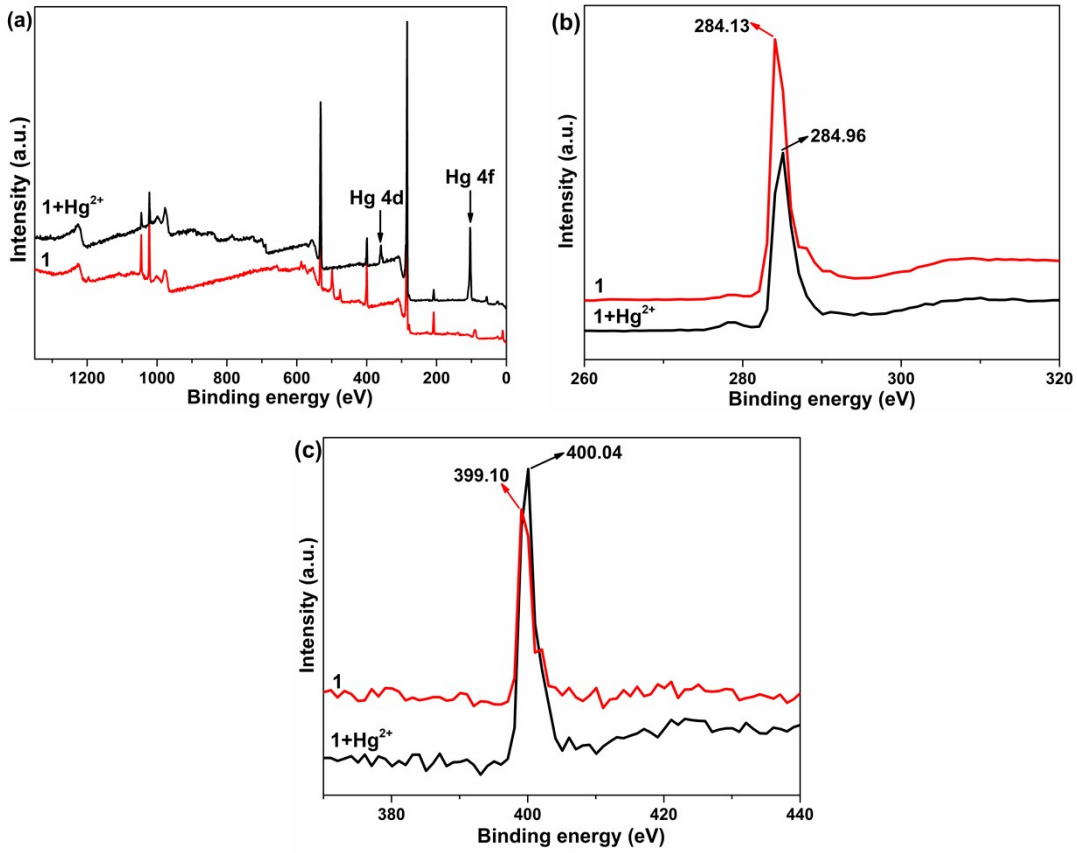

Fig. S18 (a) XPS for complex **1** and Fe^{3+} incorporating **1**; (b) C 1s XPS for **1** and Fe^{3+} incorporating **1**; (c) N 1s XPS for **1** and Fe^{3+} incorporating **1**.

Section 4 Detection of nitro explosives

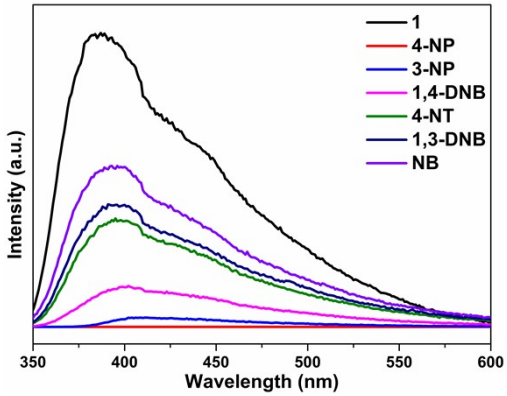

Fig. S19 Luminescent spectra of **1** before and after detection of different nitro complexes at room temperature (Condition: 5 mg **1**, 3 mL DMF and 20 μL analyte solvent (0.2 M)).

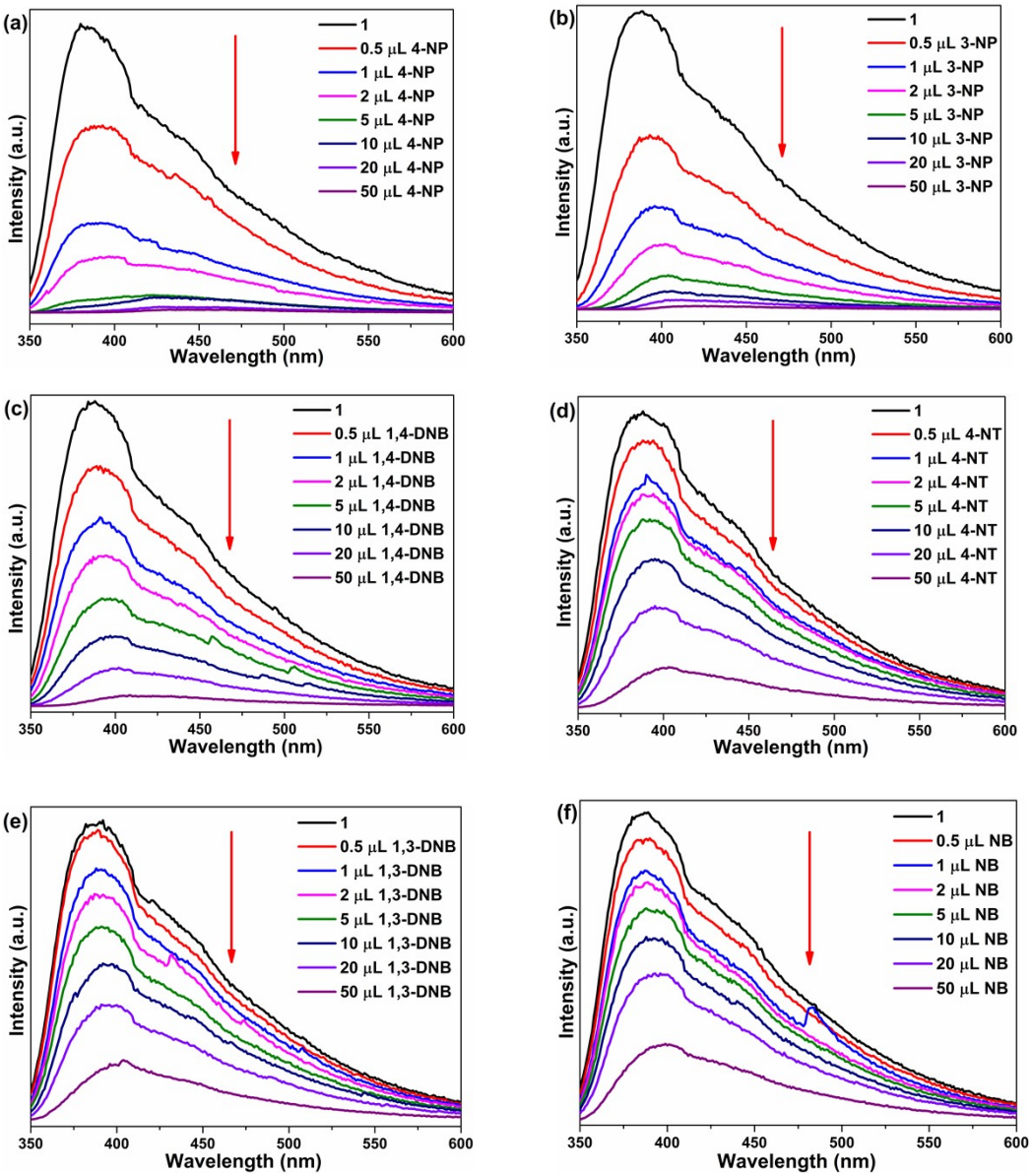

Fig. S20 Fluorescent spectra of **1** suspension (1.67 mg/mL) upon incremental addition of nitro compounds (0.2 M).

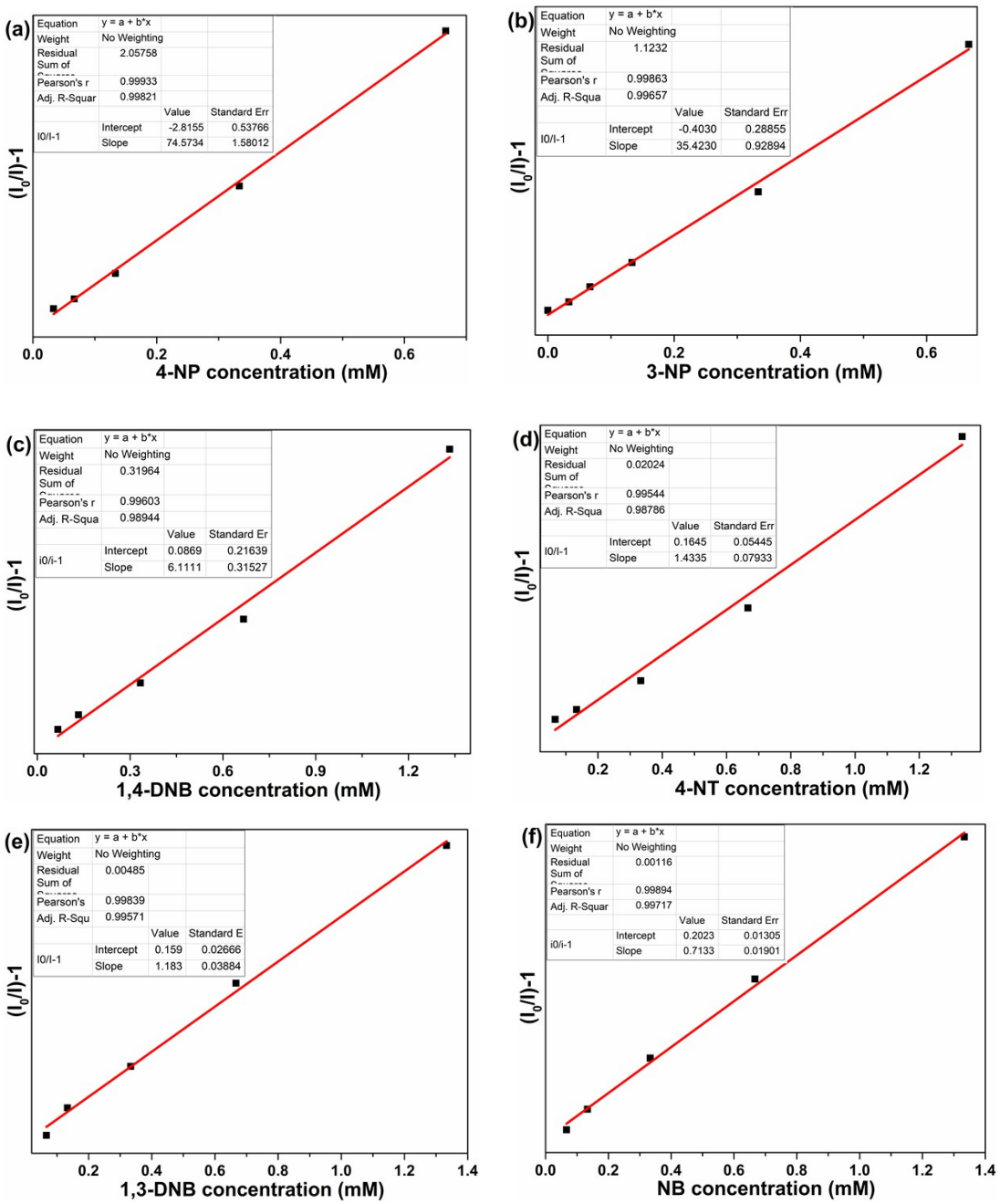

Fig. S21 S-V plot of **1** suspended in DMF (1.67 mg/mL) upon incremental addition of nitro compounds (0.2 M).

Table S6 Quenching effect coefficients (K_{sv}) of nitro compounds effect on the luminescent intensity of molecule incorporated **1**.

No.	Nitro compounds	K_{sv} (M^{-1})
1	4-NP	7.46×10^4
2	3-NP	3.54×10^4
3	1,4-DNB	6.11×10^3
4	4-NT	1.43×10^3
5	1,3-DNB	1.18×10^3
6	NB	0.71×10^3

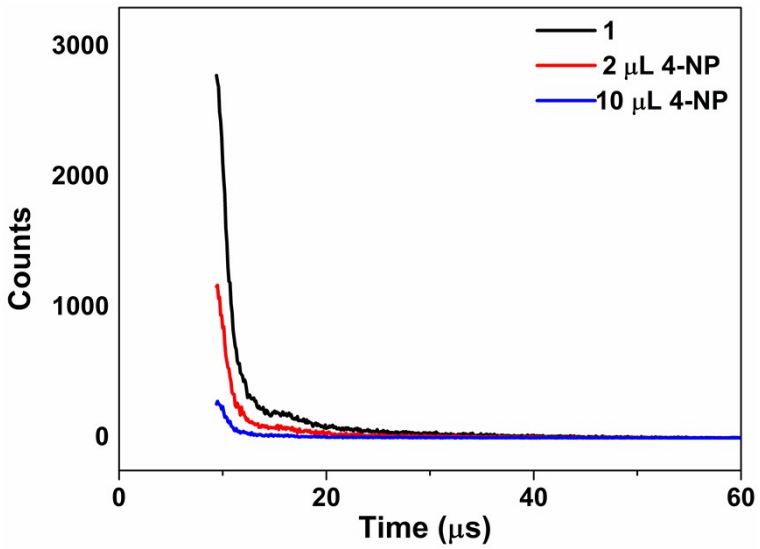

Fig. S22 The fluorescence decay curves of **1** in 4-NP solution (0.2 M).

Table S7 Average fluorescence lifetime (<τ>) values of **1** before and after addition of 4-NP

4-NP (μL)	a_1	a_2	τ_1 (μs)	τ_2 (μs)	<τ> (μs)	χ^2
0	3.64	0.28	1.17	9.67	4.47	1.14
2	1.46	0.12	1.00	8.46	4.06	0.98
10	0.34	0.03	1.19	8.19	3.83	1.06

$<\tau> = (a_1\tau_1^2 + a_2\tau_2^2)/(a_1\tau_1 + a_2\tau_2)$

To calculate the standard deviation and detection limit of this detection method, 5 mg **1** was well ground and suspended in 3 mL DMF, respectively. Then, 4-NP solution (5 mM, 0.5-10 μL) was added into the suspension and the fluorescent intensities were recorded. Standard deviation (σ) was calculated from five blank tests of **1** suspension, and the detection limit was calculated via the formula: 3σ/k (k: slope of the straight line).

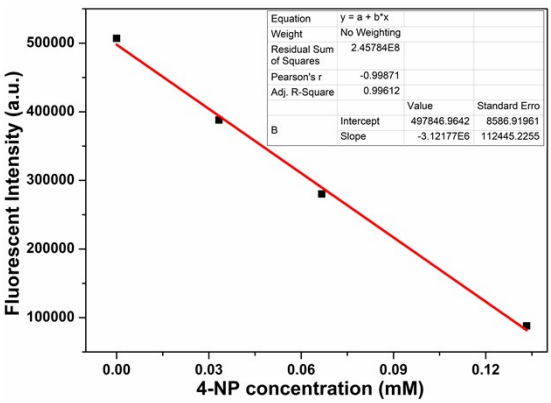

Fig. S23 Linear curve of fluorescent intensity of **1** suspension upon incremental addition of 4-NP.

Table S8 Standard deviation calculation for **1**

Compound **1**	Fluorescent intensity ($\times 10^5$)
Test 1	5.170
Test 2	5.165
Test 3	5.162
Test 4	5.173
Test 5	5.171
Standard deviation (σ)	0.0045

Table S9 Detection limit calculation of **1** for 4-NP

Compound **1**	
Slope (k)	3.122×10^6 mM^{-1}
Detection limit (3σ/k)	0.000432 mM

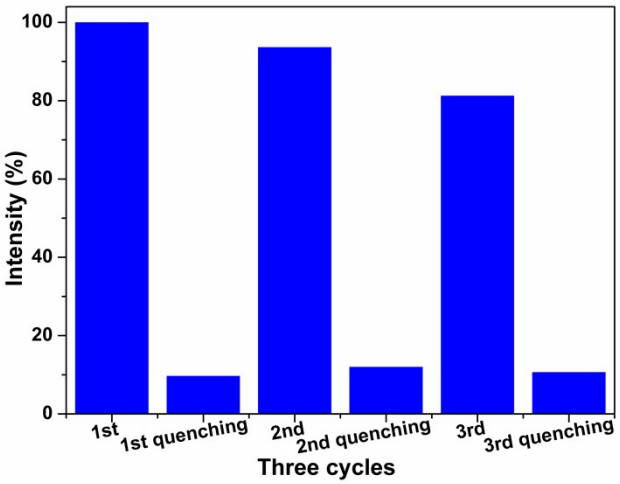

Fig. S24 Three quenching cycles of **1** suspension with the addition of 4-NP solution.